IV.A.5 Investigations of Cr Contamination in SOFC Cathodes Using TEM

Prof. Paul A. Salvador (Primary Contact)
and Dr. Shanling Wang
Carnegie Mellon University
Department of Materials Science and Engineering,
5000 Forbes Ave.
Pittsburgh, PA 15213
Phone: (412) 268-2702; Fax: (412) 268-7596
E-mail: paul7@andrew.cmu.edu

DOE Project Manager: Lane Wilson
Phone: (304) 285-1336
E-mail: Lane.Wilson@netl.doe.gov

Collaborators:
Dr. Michael Krumpelt and Dr. Terry A. Cruse
Argonne National Laboratory (ANL)
9700 South Cass Avenue
Argonne, IL 60439-4837
Phone: (630) 252-8520; Fax: (630) 252-4176
E-mail: krumpelt@cmt.anl.gov

Objectives

- To develop a straightforward sample preparation method using a focused ion beam (FIB) to produce transmission electron microscopy (TEM) specimens from specific regions of solid oxide fuel cells (SOFCs) exposed to different operating conditions.
- To carry out TEM investigations on SOFCs provided by ANL collaborators to determine the local microstructure/chemistry associated with Cr contamination.
- To understand better the mechanism of Cr contamination in the active (mixed) cathode region of SOFCs.

Accomplishments

- Developed FIB technique to reliably produce TEM specimens from the mixed lanthanum strontium manganate/yttria-stabilized zirconia (LSM/YSZ) (or active) cathode region of SOFCs, either under the flow channel or under the contact (landing) in ribbed interconnects.
- Determined the local microstructures and Cr-containing phases in various regions of six different fuel cells, each run for 500 hours but each run under different operating conditions (temperature and current density).
- Analyzed chemical composition and crystal structures of Cr-containing phases using energy dispersive spectroscopy (EDS), electron energy loss spectroscopy (EELS), selected area electron diffraction (SAED), and scanning transmission electron microscopy (STEM).
- Demonstrated that the highest contamination points were directly under the interconnect contact and near the electrolyte; evidence of contamination decreased quickly away from these areas.
- Established the signature of degradation as the existence of nanoparticles (d<100 nm) on solid surfaces (YSZ and/or LSM); the local number density, size, and chemical composition of such nanoparticles are factors of location, temperature, and current density.
- Clarified the mechanism of Cr contamination for SOFCs run at 700°C.

Introduction

Ferritic stainless steel alloys have been considered as interconnect materials in SOFCs whose operating temperature is in the 600-800°C range, since steels are relatively inexpensive and are stable in these conditions. However, in hydrated oxidizing atmospheres at these temperatures, Cr is volatile and forms several vapor species, such as $CrO_2(OH)_2$. It is well known that, without the use of effective protective coatings on the steel, the gaseous Cr species can react with cathode components (in LSM/YSZ cathodes) and can cause rapid degradation of SOFC performance. While coatings may effectively reduce the vapor pressure of Cr species, it is still important to understand the mechanism by which Cr contamination occurs in the SOFC cathode and to establish operating conditions in which the degradation levels are acceptable for a given vapor pressure. There are considerable disagreements on the mechanism(s) by which Cr species react with the cathode components.

This work aims to determine the precise mechanism of Cr contamination. To do so, we have carried out TEM investigations of SOFCs operated (at ANL) under different conditions to better understand the nanoscale microstructural/chemical properties at different stages of Cr contamination. This project is part of a larger effort led by the group at ANL to understand SOFC degradation as a function of operating conditions. At ANL, cells were operated in various fuel cell conditions and were characterized electrochemically as well as microstructurally using scanning electron microscopy (SEM), EDS, and high-energy X-rays at the Advanced Photon Source (APS). TEM complements these spatially averaging techniques by allowing us to locate nanosized

grains and interrogate their precise chemistry/structure; for low levels or the initial stages of contamination, TEM allows us to identify the location and nature of Cr contamination. The results will ultimately allow us to determine how SOFC interconnects/cathodes can be optimized to meet DOE program goals.

Approach

Anode (Ni/YSZ) supported single cells (8YSZ electrolyte and LSM/8YSZ active [mixed] cathode) were purchased from InDEC and operated under various conditions: 700°C and 800°C at several current densities. E-BRITE® interconnects were used for current collection on the cathode, and provided the source of chromium. Between the interconnect and the active cathode, an LSM contact paste was applied. In some cases, Au foil was wrapped around regions of the E-BRITE® interconnect to block Cr migration pathways. Such single cell SOFCs were run for 500 hours each and the operating conditions, such as temperature and current density, were varied between cells.

To determine the local nature of Cr-poisoning in these cells, we developed a cross-sectional TEM specimen fabrication method using a FIB that enables us to locate and later image precise positions in the LSM/YSZ active cathode. TEM, STEM, EDS, chemical mapping, EELS, and SAED techniques were used to analyze chemical composition and crystal structures of the Cr-containing phases and to investigate how degradation occurred under the given operating conditions.

Results

TEM specimens from different locations in the active (mixed) cathode of different fuel cells were studied. In this report, based on the observations made of many cells using TEM, we define degradation as the observation of changes from the original cathode microstructure, the observation of nanoparticles ($d<100$ nm), and the observation of Cr in solid phases. Figure 1 gives examples of a degradation-free cell (1a) and a severely degraded cell (1b), which are discussed more below.

Cell numbers ANL-35, 36, and 37 were each operated at 700°C under the "standard" current density (1.15 A), but with different types of interconnects. For the interconnect, ANL-35 had E-BRITE®, ANL-36 had E-BRITE® that was Au-wrapped in a manner where the landings were covered but the flow channels were exposed, and ANL-37 had E-BRITE® that was Au-wrapped in a manner where such that no E-BRITE® was exposed. No degradation was observed under regions that were protected with Au foil (i.e., in the landing region of ANL-36 or anywhere in ANL-37).

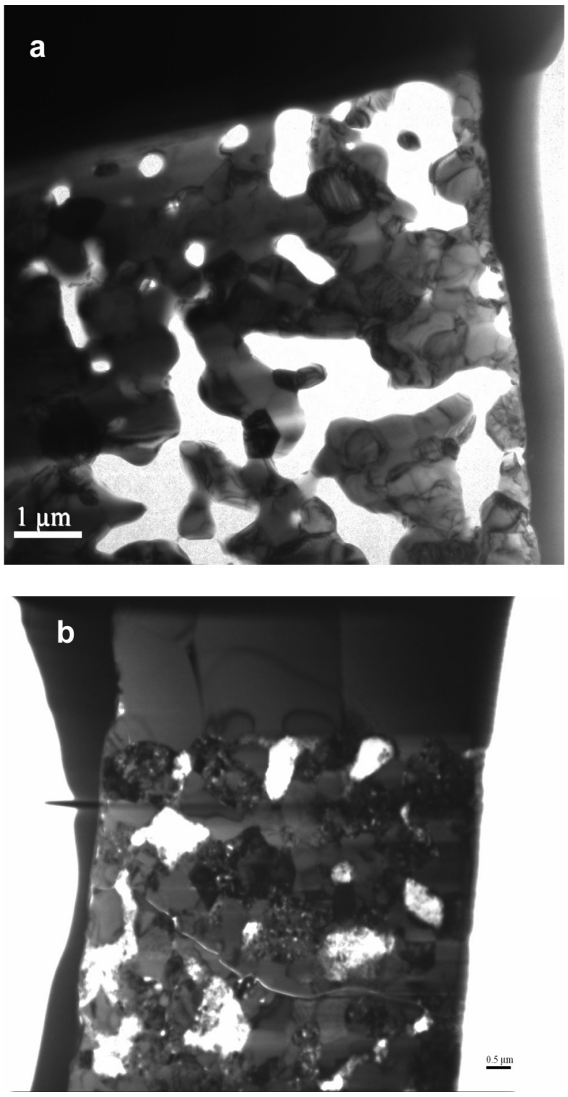

FIGURE 1. Bright-Field TEM Images Showing Active LSM/YSZ Cathode Microstructures for Different Fuel Cells: (a) ANL-36 with No Degradation and (b) ANL-35 with Massive Degradation Under the Interconnect Landing

Furthermore, no degradation was observed in ANL-36 under the exposed channel (as seen in Figure 1a), implying that the Au on the landing sufficiently protected the cell under these conditions. For other ANL fuel cells with exposed E-BRITE® interconnect landings, including ANL-35, degradation was observed throughout the cell. Figure 1b shows the massive degradation below the landing in ANL-35 (discussed further below), in which the pores are largely filled with nanoparticles and some pre-existing grains of LSM have decomposed. It should be noted that no microstructural degradation was observed in the porous-LSM contact paste region of the cathode, and the extent of degradation in the active LSM/YSZ region depended strongly on the location (landing or channel

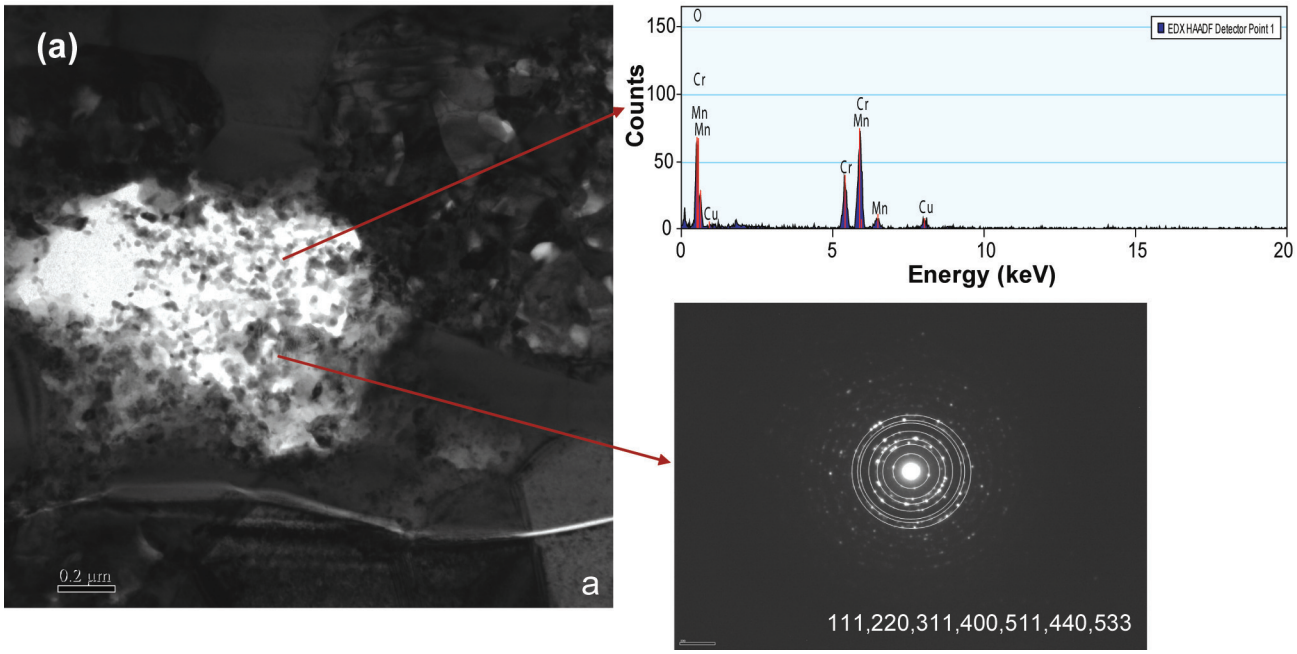

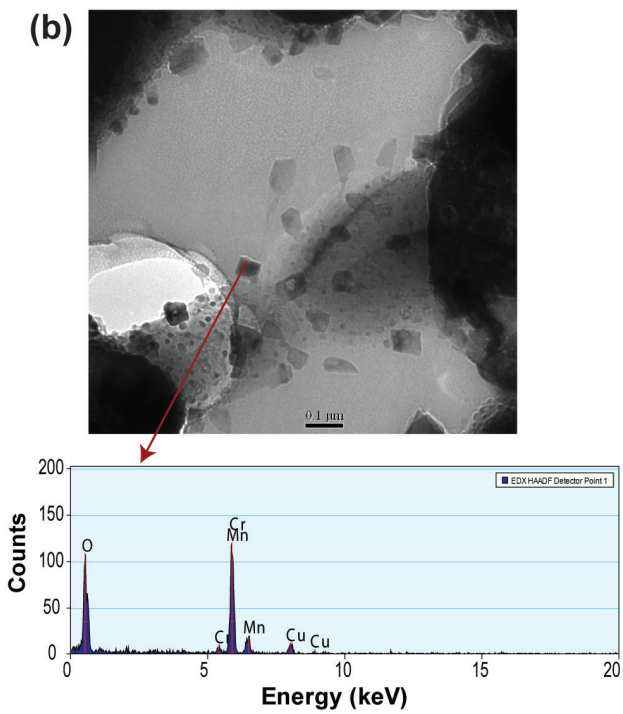

FIGURE 2. (a) Bright-field TEM image, EDS spectrum, and SAED showing degradation microstructures for ANL-35 under the landing. The EDS and SAED pattern of nanoparticles correspond to (Cr, Mn)$_3$O$_4$. (b) Similar images for ANL-35 under the channel.

and proximity to electrolyte), temperature, and current density.

For fuel cell ANL-35, two different degradation rates were observed under the landing and channel (Figure 2), respectively. Under the landing (Figure 1b and Figure 2a), nanoparticles filled the pores of LSM/YSZ region and LSM was almost completely decomposed. SAED in TEM demonstrated that the nanosized materials in the pores were crystalline and their diffraction pattern was consistent with the spinel structure ($Mn_xCr_{3-x}O_4$) (Figure 2a). Under the flow channel, Cr-poisoning was observed to a much less extent than in the similar region under the interconnect landing, owing to the fact that the Cr-containing vapor species appear to be removed by oxidant flow in the channels (similar to the lack of degradation in ANL-36 under the flow channels). A significant number of individual nanoparticles were observed to occur on the YSZ-pore boundaries (under the flow channel), with no obvious LSM in contact with them. These particles contained Cr and Mn, but no Y or Zr. The solids that most of the nanoparticles decorated contained Y and Zr, but no Cr or Mn. This strongly indicates that the YSZ surfaces are prone to coverage by $(Cr,Mn)_xO_y$ solids at low levels of degradation (see Figure 2b).

SOFC ANL-43 was operated in conditions similar to ANL-35 but using half the standard current density, or 0.575 A. Electrochemically, the cell experienced little degradation and one expects that the levels of Cr contamination under the landing and flow channel will decrease as well. In fact, the degradation observed under the landing of ANL-43 was similar to that observed under the flow channel of ANL-35, in line with expectations. As shown in Figure 3, a significant amount of Cr and Mn was found on the surface of the YSZ particle. At the boundary between YSZ and LSM, there are some phases that contain less Mn (the black spots) and, more importantly, there were no Cr-containing phases observed across the boundary on the LSM particle. These results imply that the initial stages of the

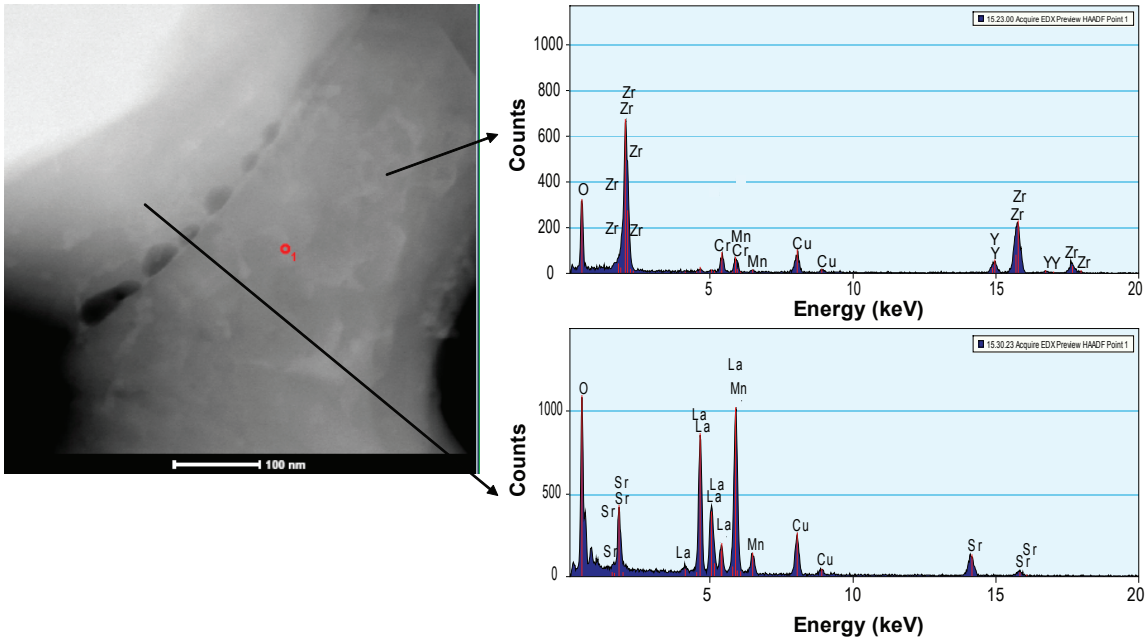

FIGURE 3. STEM Image (Left Panel) Showing Active LSM/YSZ Cathode Boundary Microstructures for ANL-43, with Two EDS Patterns from the Marked Regions (Above a YSZ Grain for the Top Right Panel and Above a LSM Grain for the Lower Right Panel)

deposition of gaseous Cr species occur on YSZ surfaces that contain Mn species (generated under cathodic polarization and high temperatures) as Cr-Mn-O nuclei. This is likely followed by LSM decomposition that begins at LSM/YSZ boundaries having YSZ coated with Cr-containing solids. Other images showed that YSZ particles that had Cr-containing solids had some regions with Mn containing solids, but also had local regions that appeared Mn-free. This implies that Mn plays a role in nucleation but growth can occur without Mn present.

Figure 4 shows the nanoparticles' microstructures for ANL-31. This cell was similar to ANL-35 (having exposed to E-BRITE® and operated at 1.15 A), but ANL-31 was run at 800°C instead of 700°C. ANL-31 exhibited a different structural degradation and a lower electrochemical degradation. The structural degradation occurred in the active LSM/YSZ region of the cathode. Three different types of particles were found; MnO_x (on LSM), Cr_2O_3, and $(Cr, Mn)_3O_4$ particles were all found. SAED showed that the most of the particles (which covered most of the regions) are of the Cr_2O_3 type. These results imply that the mechanism of Cr-contamination is different at these two temperatures.

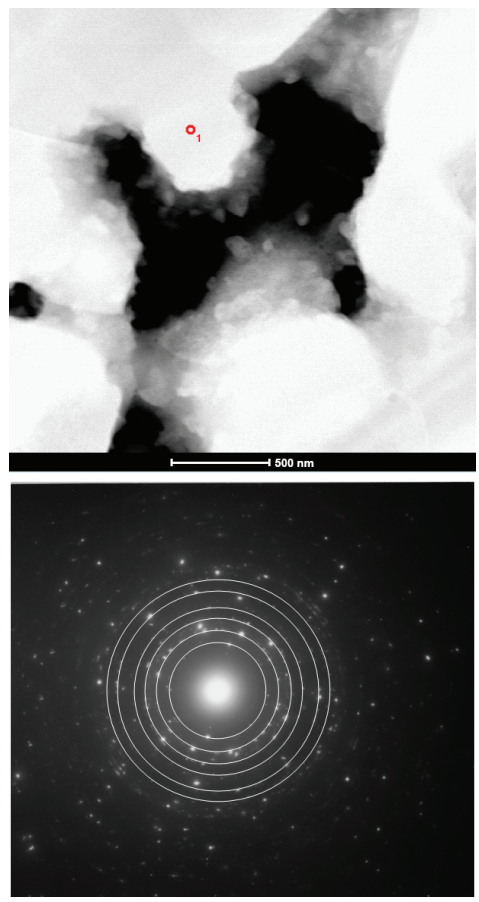

FIGURE 4. Bright-field image showing the active LSM/YSZ cathode microstructures for ANL-31 under the landing. The SAED pattern and EDS spectrum of the nanoparticles correspond to Cr_2O_3 type.

Conclusions and Future Directions

The microstructures of LSM/YSZ active cathode region of ANL fuel cells under different operating conditions were studied by analytical TEM, and the local position, chemical composition and crystal structure of Cr-containing nanoparticle phases were determined. All results were consistent with earlier observations made

at ANL but these allowed for the local distribution of phases on individual particles to be ascertained. The Cr-poisoning mechanism was established for cells operated at 700°C; which demonstrated that Mn-species covered YSZ and participated in the early stages of Cr-deposition. Later stages were likely more complex, but included the complete decomposition of LSM grains. Future work will further confirm this model and will explore the degradation mechanisms at other temperatures and using other electrochemical operational parameters.

FY 2007 Publications/Presentations

1. Contributed images to: "Degradation of SOFCs in Contact with EBrite," T. A. Cruse*, M. Krumpelt, B. Ingram, and D. Liu, presented at "4th International Symposium on Solid Oxide Fuel Cells (SOFC)," at 31st International Cocoa Beach Conference & Exposition on Advanced Ceramics & Composites, Daytona Beach, January 21-26, 2007.

2. Contributed images to: "Microtexture of SOFC Cathodes Subjected to Thermal and Electrochemical Loads," Y. Cao, H. M. Miller, C. Johnson, L. Wilson, P. Salvador, and G. S. Rohrer*, presented at "4th International Symposium on Solid Oxide Fuel Cells (SOFC)," at 31st International Cocoa Beach Conference & Exposition on Advanced Ceramics & Composites, Daytona Beach, January 21-26, 2007.